Available online at www.sciencedirect.com

jmr&t Journal of Materials Research and Technology

journal homepage: www.elsevier.com/locate/jmrt

Original Article

Extraction and characterization of nanocellulose from three types of palm residues

Sherif Mehanny [a], *Ehab E. Abu-El Magd* [c], *Maha Ibrahim* [c], *Mahmoud Farag* [d], *Rodrigo Gil-San-Millan* [b], *Jorge Navarro* [b], *Abd El Halim El Habbak* [a], *Emad El-Kashif* [a,*]

[a] *Mechanical Design and Production Department, Faculty of Engineering, Cairo University, Cairo University Rd, Giza, 12613, Egypt*

[b] *Department of Inorganic Chemistry, Faculty of Science, University of Granada, Fuente Nueva, Granada, 18071, Spain*

[c] *Cellulose and Paper Department, National Research Center, El-Tahrir St., Dokki, Giza, Egypt*

[d] *Department of Mechanical Engineering, School of Sciences and Engineering, The American University in Cairo, New Cairo, Cairo, 11835, Egypt*

ARTICLE INFO

Article history:
Received 29 July 2020
Accepted 7 December 2020
Available online 13 December 2020

Keywords:
Nanocellulose
Lignin containing
Acidic hydrolysis
Palm
Residues
Valorization

ABSTRACT

Carbon footprint and nonrenewability are among the motives to mitigate dependence on oil resources. On the other hand, palm trees exceeded 100 million around globe, which poses enormous amount of biowastes to get exploited per annum. Moreover, nanocellulose is emerging as efficient low cost material, which shows increasing versatility throughout time. In this investigation we will attempt to extract nanocellulose from palm wastes (fronds, leaves, and coir), and characterize them. Dry biomass was pulped by being subjected to 10% (wt/wt) NaOH alkaline treatment at 160 °C for 2 h. Pulped non-bleached biomass underwent acidic hydrolysis by mechanical stirring in 20% H_2SO_4 (v/v) and heating to 120 °C for 30 min. After filtration, neutralization, and centrifugion, resultant particles were characterized to assess their morphology, size, particle charge, existing chemical groups, and crystallinity. For the three types of palm residues, our preparation technique was successful to isolate lignin containing nanocellulose particles. However, coir was more recalcitrant to acidic hydrolysis than fronds and leaves. Our palm residues yielded 42 −82 nm spherical particles, and zeta potential ranging between −11 and −19 mV. Crystallinity was higher after pulping, and lower after hydrolysis, which suggests promotion of amorphous content of cellulose. Lignin-containing nanocellulose prepared in this study initiates promising horizon especially in heavy metal (cations) removal from water in environmental applications and sustained drug delivery for medical applications.

* Corresponding author.
E-mail address: eelkashif@yahoo.com (E. El-Kashif).

https://doi.org/10.1016/j.jmrt.2020.12.027

1. Introduction

During recent decades, increasing environmental awareness incited many governments, institutions, and firms to reduce fossil fuel consumption. Carbon footprint and resource non-renewability are amid the fundamental reasons to lessen dependence on petroleum resources. In the same context, lignocellulosic biomass emerged as reliable alternative for petroleum based plastics. Lignocellulosic biomass is estimated to be the most widely spread biopolymer on earth. Global annual production of this biopolymer is roughly calculated to be 1.3×10^{10} metric tons [1]. Lignocellulosic biomass encompasses: 1) agriculture wastes (palm residues, empty fruit bunch, straw, bagasse, corncob, Nile rose and stover) [2–5], 2) forest wastes (branches, unwanted stems, and withered leaves) [6], and 3) industrial wastes (waste paper, and demolished wood) [7]. Ample of lignocellulosic residues and their capacity to act as a "carbon sink", promoted their use in more than 200 applications, comprising construction materials, moderate strength composites, adhesives, packaging, coatings, dental fillings, implants, and drug delivery [1,8].

Palm is considered rich source of lignocellulosic biomass. Around the globe, more than 120 million palm tree comprising 12 millions in Egypt [9]. Annually, each tree produces 20–30 kg of wastes at least, which poses significant problem in case those residues were not dealt with in ecofriendly manner [10, 55].

Cellulose is not exception from other materials grabbing interest; when new procesminiaturized to nano scale, unexpected properties are observed. After extracting nanoscale cellulose porous structure, 51–531 $m^2.gm^{-1}$ specific surface area were reported [11].

Nanocellulose extraction is a good way to valorize palm wastes and exploit them in versatile application. Nanocellulose is a good magical particle which receive ever increasing interest during last 2 decades. Its applications includes composites fabrication, paper modification, packaging, and biomedicine [12]. Nanocellulose mechanical properties are non negligible asset, tensile strength of nanocellulose exceeds 10 GPa (10 times of steel), its tensile modulus averages to 130 GPa, despite its low density (1.5–1.6 $gm.cm^3$) [13]. Low thermal expansivity and capacity to form transclucent films (particle smaller than light wave length), in addition to vapor and O_2 barrier properties, and most importantly biocompatibility (or biodegradability) enabled nanocellulose to become versatile material in multitude of applications [14–16]. Polymeric composite reinforcement and paper (board) strengthening are direct applications to high mechanical properties [17,18]. Barrier properties in addition to mechanical properties, and biodegradability make nanocellulose perfect match for packaging solutions [19]. Moreover, nanocelluose have well-proven and promising role in developing construction, energy, and electronics industries [20].

Nanocellulose can be extracted via three routes. First one is chemical extraction, in which acid attacks amourphous regions of the celluloseic structure leaving cellulose nano crystals (CNC). Second one is mechanical extraction. Mechanical work is exerted to disintegrate the cellulosic hierarchy, yielding cellulose nanofibrils (CNF). Third method is bacterial extraction, in which bacteria assemble glucose monomers in long cellulose chains, yielding bacterial nano cellulose (BNC) [21]. Most researchers concentrate on the fabrication and application of lignin-free cellulose-based materials for mature technology and green properties [22]. However, extracting cellulose from lignocellulose biomass requires series of harsh purification processes, generating undesirable byproducts [23]. Contrarily, preparation of lignin-containing solutions can limit the consumption of bleaching chemicals and energy, and thus, the use of lignin-rich material is more environmentally-friendly and less costly than using bleached material. Furthermore, lignin, the most abundant natural aromatic polymer (more than 30% of biosphere [24]), can perform as a binder to glue cellulose and hemicellulose, imparting the strength and rigidity of woody plants [25,26]. It comprises numerous chemical groups, such as phenolic hydroxyl, methoxyl, and carboxyl groups, which can play as active sites for adsorption of dyes and metal cations. Lignin also has other properties as antimicrobial, antioxidant properties and high thermal stability [27]. Therefore, we can hypothesize that lignin containing nanocellulose can provide unique properties.

In this article, we will investigate lignin containing nanocellulose extracted chemically from 3 types of palm residues; namely, fronds, leaves, and coir (palm stem mesh).

2. Experimental

2.1. Materials

Three types of palm residues; namely, fronds, leaves, and coir were collected from palm farming land located in Minia Governorate, Egypt. Fronds only were received as powder, wheras the other types were native (nonchopped).

2.2. Preparation

All types of palm residues were washed thoroughly. Non chopped residues were cut into pieces and subjected to grinding process using home use mixer. Pulping process was performed by mixing 100 gm of biomass with 1L of 10% NaOH (wt/wt), mixture heated up to 160 °C for 2 h, and then fibers were washed thoroughly and dried in open air. Pulped fibers were finally subjected to acidic hydrolosis, 10 gm of pulp 200 ml of 20% H_2SO_4 (v/v) and heated to 120 °C for 30 min with stirring, as conducted elsewhere [54]. After brownish paste like texture shows up, 1500 ml of frozen distilled water was added to quench the reaction. Afterwards suspension was poured onto 0.22 μm Millipore filter for 24 h. Concentrate cake was neutralized by 5% w/v $NaHCO_3$ until pH of 7–8. Subsequently, resulting suspension was centrifuged at 6000 rpm for 15 min. Following that, supernatant was decanted and replenished by dI water. The 50 ml tube was shaken and recentrifuged. Eventually the last 2 steps were repeated 1–2 times until pH 7.

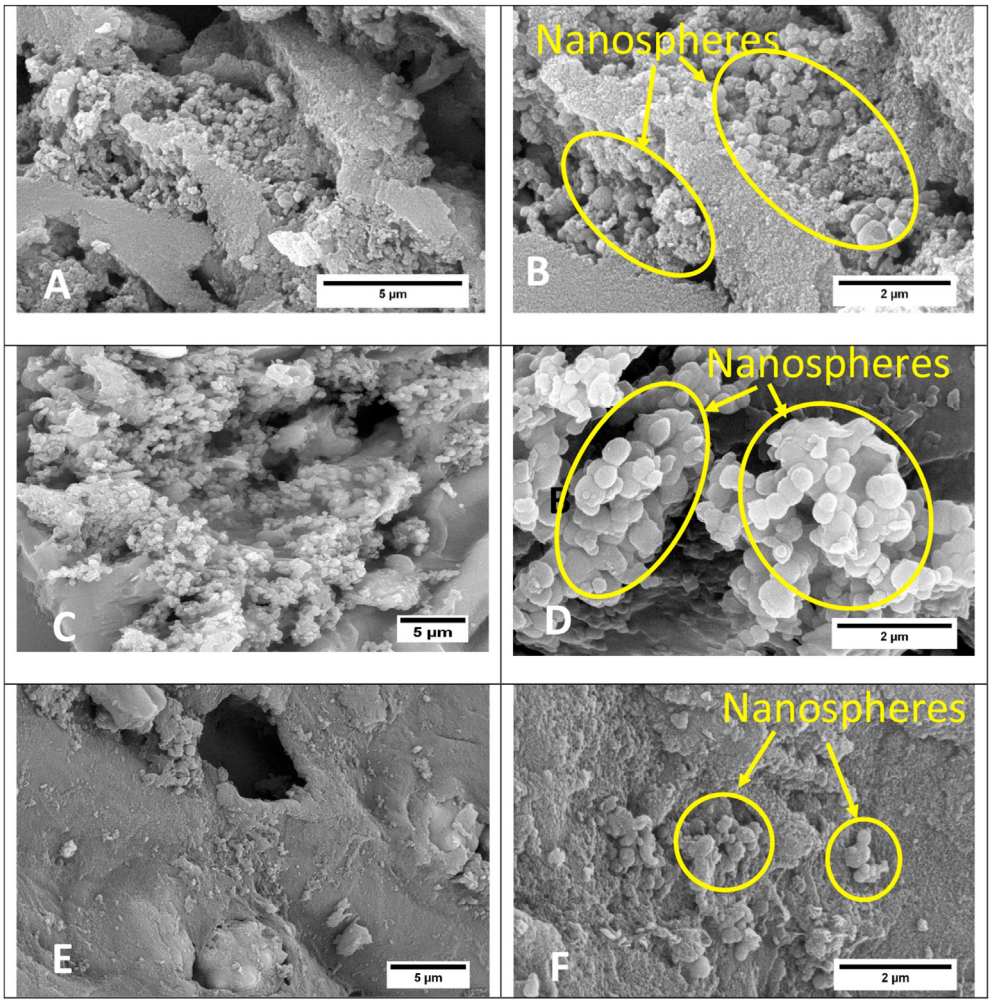

Fig. 1 – SEM illustration of nanocellulose extracted from 3 types of palm residues; A & B nanocellulose from palm fronds, C & D nanocellulose from palm leaves, and E & F nanocellulose from palm coir. B, D, & F are magnified figures from A, C, & E. Agglomerates of cellulose nanospheres are encircled or pointed to by yellow lines.

2.3. *Characterization*

2.3.1. *SEM analysis*

The morphological structure of chemical treated biomass was investigated using Scanning Electron Microscope (SEM, FEI Quanta FEG 250, FEI Corp). Dry powder sample was placed on carbon tapes and then sputtered with thin gold layer under argon atmosphere.

2.3.2. *TEM analysis*

Transmission electron microscopy was performed using TEM 902 Carl Zeiss system (Meditec, Inc., Oberkochen, Germany). Beforehand, samples were prepared in 1: 2 water: ethanol, then bath sonicated for 13 min. Ethanol was added to speed up volatilization of liquid from the grid.

2.3.3. *Particle size distribution*

The average diameter, the size distribution, and zeta potential of samples were measured by using a particle size analyzer (Nano-ZS, Malvern Instruments Ltd., UK). For measuring zeta potential, the samples were diluted (5 times) by deionized water just before assessment.

2.3.4. *FTIR analysis*

Infra red spectroscopy was performed using FTIR spectrometer (TENSOR 27, Bruker Corp.) in the range between 4000 and 400 cm^{-1}, and 2 cm^{-1} resolution.

2.3.5. *XRD analysis*

Desktop D2 Phaser X-ray diffractometer (Bruker Corp.) with radiation at 30 kV and 10 mA was used to obtain diffractograms. Diffraction angle varied from $2\theta = 4°–40°$ with step size of 0.33°/s. Crystallinity index (CI) was calculated by formula reported elsewhere [28,29], $CI = (I_{cryst.}\text{-}I_{am})/I_{cryst}$, .where $I_{cryst.}$ is the maximum intensity in the diffractogram, most commonly at (2 0 0) peak, I_{am} is the intensity of the amorphous valley between (2 0 0) and (1 1 0), mostly at $2\theta = 18°$.

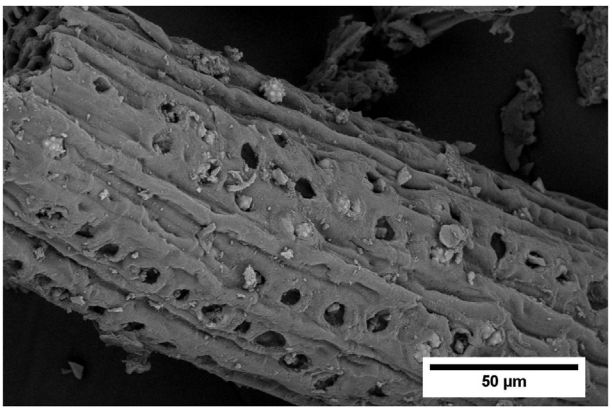

Fig. 2 – SEM for palm coir after acidic hydrolysis; it is clear that the texture was recalcitrant to hydrolysis.

3. Results and discussions

Fronds, leaves, and coir yielded 2.9, 3.01, and 3.58 gm, respectively. Sizes and morphologies of nanocellulose extracted from the three types of palm residues, were depicted by SEM and TEM in Figs. 1 and 2, respectively. Keep in mind that SEM investigation is performed on dry powder sample. The three types of residues nanocellulose (fronds, leaves, & coir) illustrated in Fig. 1 show spherical morphology, of sizes ranging between 200 and 300 nm. Fronds based nanocellulose in Fig. 1A & B, and leaves based nanocellulose depicted in Fig. 1C & D, look way more compliant to chemical reaction (acidic hydrolysis), than coir based nanocellulose (Fig. 1E & F), which exhibits recalcitrance to hydrolysis reaction. Non compliance (recalcitrance) of coir can be concluded from the clearly low number of spherical particles settling on intact coir texture (Fig. 1F). Fig. 2 exhibits zoomed out view for unmutilated coir texture despite undergoing acidic hydrolysis, which is in line with the recalcitrance phenomenon monitored in previous figure.

Although Fig. 3 displays TEM characterization of the same samples, TEM requires samples to be suspended in water/ethanol high dilution solution and sonicated. TEM showed that the three types of samples were spherical particles of average size ranging between 42 and 81 nm. Obviously, frond (Fig. 3A & B) and leaves (Fig. 3C & D) yielded significantly lower size particles than coir (Fig. 3E & F).

Images were analyzed using ImageJ tool and results were summarized in Table 1. Particle sizes monitored from TEM was substantially smaller than those of SEM. This can be interpreted by coagulations between dry particles characterized by SEM, which were splitted down by suspending in water before being pipetted on TEM grid.

Fig. 4 depicts particle size and zeta potential of fronds particles, extracted in this study. Fig. 4A shows sharp high peak around 100 nm and wide low peak (can be neglected) around 300 nm & Fig. 4B shows high sharp peak at −19 mV. Results of other particle types in this study in comparison to literature were listed in Table 2.

According to Table 4, particle size in this study falls in the range between maximum and minimum of other studies (44.7 and 350 nm). However, particles presented in this study are more inclined to neutrality (closer to 0 mV) than particles in literature, which can be affiliated to different pH and Na^+ concentration in the particles solution [30].

Fourier Transform Infra Red (FTIR) spectroscopy was performed on all samples (Fig. 5). Analysis comprised native fibers, pulped fibers, and nanocellulose, for fronds, leaves and coir. The FTIR assists us to characterize the chemical structure by identifying the functional groups present in each characterized material. Infrared spectra of cellulose, hemicellulose and lignin components were studied in previous literature [36–40]. The typical functional groups and the corresponding bands for each component are shown in Table 3 and listed elsewhere [38,39].

All materials showed main absorbance regions. The first one at low range of 700–1,800, second one at higher range between 2,700 and 3,500 approximately. Very narrow range between 2200 and 2400 wave number/cm showed up as well. Specific absorption peaks could be recognized for each particular component (Fig. 5).

For the three constituents of lignocellulosic tissue (cellulose, hemicellulose, and lignin), hydroxyl stretching vibrations are found between 3000 cm^{-1} and 3500 cm^{-1}. Majorly, peak intensity in hydrolyzed particles (CNC) was higher than non-hydrolyzed (Native), reason behind that is the lower diameter of nanocellulose, which implies larger specific area and hence larger number of hydroxyl group [41]. Peak 1 for CNC at 2890 cm^{-1} H–C–H group peak gets more intense after hydrolysis, probably because of the same reason like OH group. Peak 2 in the three plots of native residues, corresponds to aromatic groups in lignin (1700-1730 cm^{-1}). Peak 3 of native particles at 1613 or 1632 cm^{-1} corresponds to C=C in benzene stretching ring or aromatic skeletal mode for lignin texture. Peak 5 in native residues is around 1450 cm^{-1} represents aromatic skeletal ring of lignin. Peak 6 in CNC ranging between 1170 and 1082 corresponds to C–O–C group of pyranose ring skeletal in cellulose. Peak 7 in native material of the range 1047–900 corresponds to deformation vibrations of C–O bands in primary alcohol of lignin [42]. By and large, lignin peaks were sharper and more apparent in native palm residues compared to pulped or CNC; in the same context, cellulose peaks were sharper in CNC than native residues. We can deduce that pulping and hydrolysis succeeded in lignin removal from native residues. For the three types of lignin containing nanocellulose (grey curves) same listed peaks show up, but smaller and less sharp, which shows partial depletion (fading) of lignin. For instance, peak 7 in Fig. 5A (fronds), is very big and sharp, in comparison to the corresponding peaks in lignin containing CNC (small encircled peak).

Crystallinity was characterized by XRD technique, and results were showcased in Fig. 6. As explained in [44]. Cellulose diffractograms show following peaks: $2\theta = 12.5^\circ$ (for 1 1 0 plane), labeled "1" in Fig. 6, $2\theta = 15.5^\circ$ (for 1 0 1 plane), labeled "2", $2\theta = 16.5^\circ$ (for 1 0 $^-$ plane), $2\theta = 19.5^\circ$ (for 0 2 1 plane), $2\theta = 22.5^\circ$ (for 2 0 0 plane), labeled "4", $2\theta = 34.5^\circ$ (for 0 4 0 plane), labeled "5". Valley labelled "3" represents amourphous cellulose. In this investigation, all types of non-

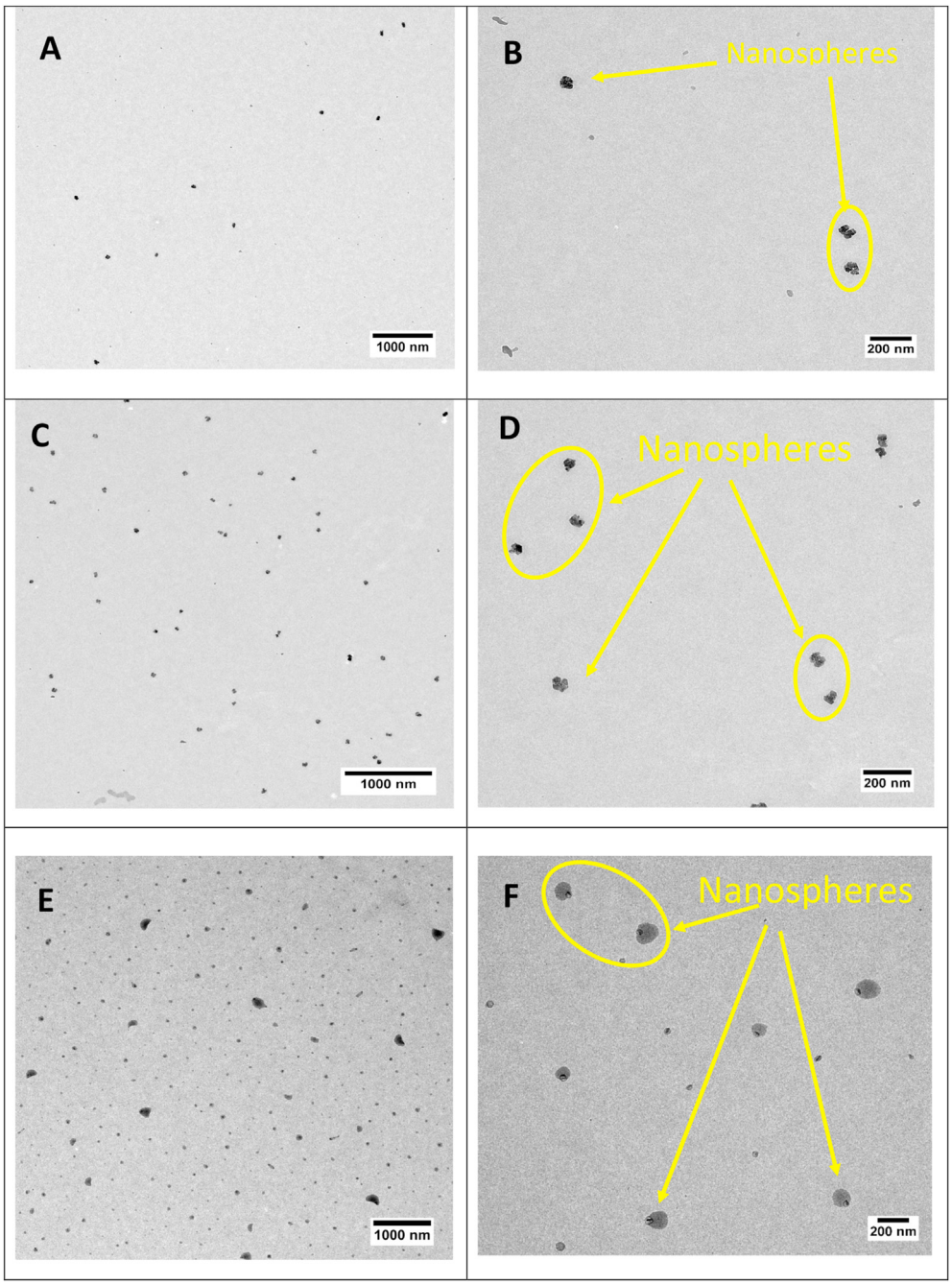

Fig. 3 – TEM illustration of nanocellulose extracted from 3 types of palm residues; A & B nanocellulose from palm fronds, C & D nanocellulose from palm leaves, and E & F nanocellulose from palm coir. B, D, & F are magnified figures from A, C, & E. Nanocellulose is encircled or pointed to by yellow lines.

Table 1 – SEM and TEM image size analysis for three types of palm residues based nanocellulose particles.

	SEM image			TEM image		
	Fronds	Leaves	Coir	Fronds	Leaves	Coir
Average size (nm)	249	320	286	42	54	81
Standard dev.	80	131	61	19.7	8.7	47
Maximum	520	660	390	73	69	158
Minimum	14	8	15	21	41	31

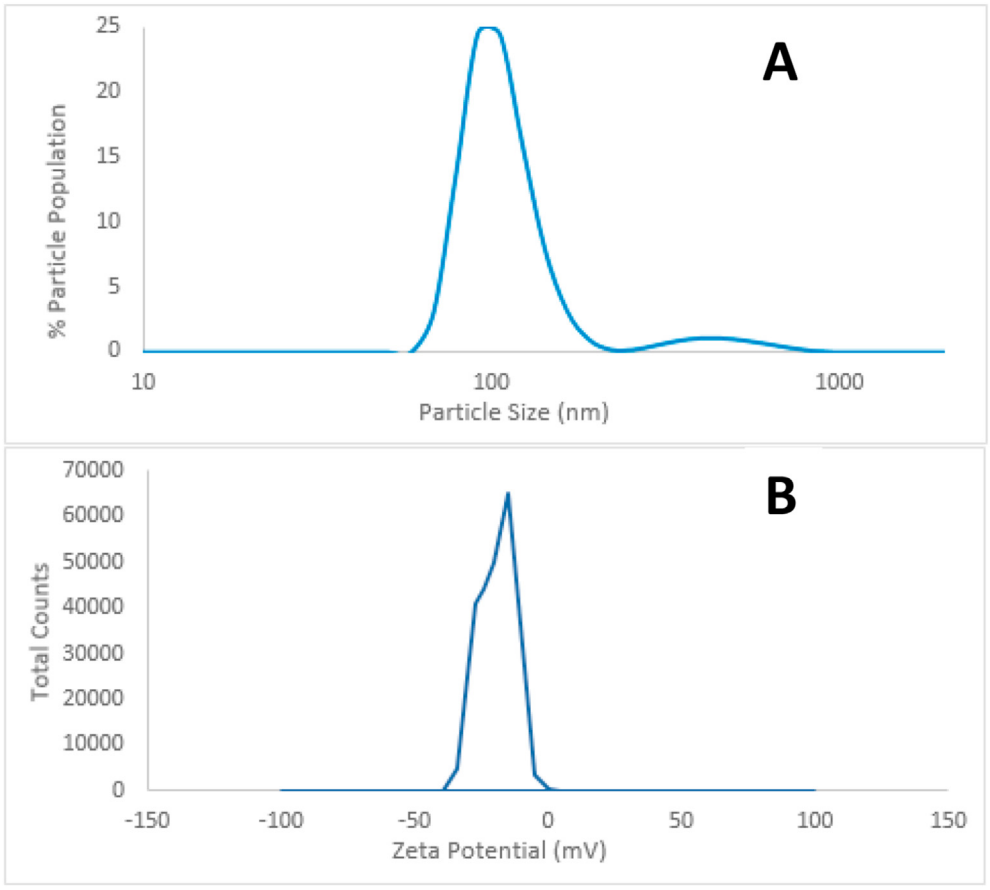

Fig. 4 – Particle size analysis of palm fronds extracted nanocellulose A), and zeta potential for the same particle type B).

hydrolyzed cellulose (native palm and pulped palm), exhibited two peaks, low one at $2\theta = 15.5$ (sometimes overlapping with $2\theta = 16.5$) and higher one at $2\theta = 22.5°$; few curves showed small peak at $2\theta = 34.5°$. Among the three types of CNC, only hydrolyzed leaves (leaves CNC) showd some sort of crystallinity, obvious through the sharp peak at $2\theta = 22.5°$. Table 4 summarizes crystallinity % of our palm residues, pulping process slightly increased crystallinity. Contrarily, hydrolysis process substantially decreased crystallynity. In other words, crystallynity peaks disappeared, indicating drastic destruction of crystalline regions, yielding amourphous structure; mentioned phenomenon was monitored elsewhere [45].

Table 2 – Zeta Potential and Particle Size of particles in this study, measured by malvern equipment, in comparison to literature.

	Zeta potential (mV)	Particle size (nm)	Ref.
Fronds NC	−18.8	108	This study
Leaves NC	−14.4	–	This study
Coir NC	−10.8	90	This study
Sigma CNC	−34	–	[30]
Sigma CNC	−53	50.3	[31]
Frond CNC	−34	44.7	[31]
Husk CNC	−35	212	[32]
Husk CNF	−25	306	[32]
Linter CNC	−45	179	[33]
Hemp Lignin	−18	–	[34]
Kraft Lignin	−60	350	[35]

Some efforts of nanocellulose extraction methods and properties are listed in Table 5. In listed literature, lignocellulosic biomass is subjected to cellulose purification process comprising pulping process (alkaline reaction) for removal of hemicellulose and partial removal of lignin. Lignin remnants are removed by bleaching process. After cellulose extraction, top-down extraction technique will be executed to break down cellulose into nanocellulose. Extraction technique can be either chemical (majorly acidic hydrolysis), or mechanical (ball milling, homogenization, & ultrasonication). Material nature and preparation technique drastically impacted properties of nanocellulose extracted.

Pulping and bleaching were executed interchangeably in literature. Few studies started with bleaching then pulping [46,47], others started with pulping then bleaching [48]. However, no study investigated effect of sorting those two processes (pulping and bleaching) on cellulose yield. Extraction of nanocellulose was performed either by acidic hydrolysis or mechanical extraction. Hydrolysis using H_2SO_4 or H_3PO_4 was executed which nanocellulose will be formed as low aspect high crystallinity nanocrystals (whiskers). Mechanical extraction using ball milling, homogenizer, or ultrasonicator yielded high aspect low crystallinity nanofibrils.

Table 3 – Absorption bands for functional groups of cellulose, hemicellulose and lignin, cited from [43].

Fiber component	Wave number (cm_1)	Functional group	Compounds
Cellulose	4,000–2,995	OH	Acid, methanol
	2,890	H–C–H	Alkyl, aliphatic
	1,640	Fiber–OH	Adsorbed water
	1,270–1,232	C–O–C	Aryl-alkyl ether
	1,170–1,082	C–O–C	Pyranose ring Skeletal
	1,108	OH	C–OH
Hemicellulose	4,000–2,995	OH	Acid, methanol
	2,890	H–C–H	Alkyl, aliphatic
	1,765–1,715	C=O	Ketone and carbonyl
	1,108	OH	C–OH
Lignin	4,000–2,995	OH	Acid, methanol
	2,890	H–C–H	Alkyl, aliphatic
	1,730–1,700		Aromatic
	1,632	C=C	Benzene stretching Ring
	1,613, 1,450	C=C	Aromtic skeletal mode
	1,430	O–CH_3	Methoxyl– O–CH_3
	1,270–1,232	C–O–C	Aryl-alkyl-ether
	1,215	C–O	Phenol
	1,108	OH	C–OH
	700–900	C–H	Aromatic hydrogen

Some other studies didn't target pure cellulose nanoparticles; instead, lignocellulose nanoparticles were prepared [49–51]. Lignocellulose nanoparticles (or lignin-rich nanocellulose) are grabbing more attention due to proven higher capacity to adsorb heavy metals and to deliver drug molecules, properties which were backed by amorphous texture or lignin, its aromatic (phenolic) nature, and negative charge surface. Lignin-rich nanocellulose can be produced by enzymatic hydrolysis, in which cellulase degrade parts of cellulose yielding lignocellulose particles [50], or by skipping bleaching process so that lignin ramnants stay within texture [49]. Sulfonation process introduces sulfonate groups to lignin, by using sulfuric acid or sodium sulfite, yielding lignosulphonates [52]. Lignosulphonates are reliable sequestering particles that trap different metal ions as iron, calcium, copper, nickel, aluminum and zinc. Thus, lignosulfonates solutions can be implemented in treatment of soils by either adding deficient minerals or absorbing harmful metals [53].

In this study, three types of palm based non bleached nanocellulose were extracted by alkaline pulping, directly followed by acidic hydrolysis, which suggests that particles extracted are lignin-rich nanocellulose.

In showcased literature, acidic hydrolysis yielded cellulose nanowhiskers of width ranging between 4 and 23 nm, depending on acid concentration, and whether fibers were subjected to mechanical disintegration after hydrolysis or not. Lignin-containing cuboidal particles were prepared of sizes ranging between 50 and 100 nm [50]; this is the most resembling size and morphology to extracted particles in this study, which ranged between 42 and 81 nm. Dark color and non-rod like structure indicate that lignin is contained in the texture.

In literature and this study, FTIR peaks of –OH group increased and got sharpened after nanocellulose extraction, this is attributed to the smaller size of resultant particles, which leads to larger number of OH group attached to fiber surfaces. Lignin peaks disappeared after pulping (and bleaching), which was quite clear in nanocellulose peaks. Contrarily, cellulose peaks were sharper and higher after treatment and nanocellulose extraction.

XRD diffractograms of listed literature showed higher crystallininty for pulped fibers than native. Which is expected due to partial removal of lignin, and crystallinity even increased after nanocellulose extraction. Lani et al. [46] reported increase in crystallinity from 38 to 73%, whereas Elias et al. [47] reported increase from 23 to 70%, and Franco et al. [48] reported increase from 21 to 50%. Increase in Franco report was way lower than other literature, because cellulose was extracted as fibrils not crystals. Rangan et al. [50] reported decrease in crystallinity from 68 to 51%, which is due to enzymatic hydrolysis of cellulose and boosting up percentage of lignin. In this study, crystallinity increased after pulping, and decreased or even vanished after hydrolysis. This is because avoiding executing bleaching process, which necessates presence of lignin within texture; acidic hydrolysis might didn't target lignin in particular, contrary in transformed crystalline cellulose to amorphous structure.

Table 4 – Crystallinity % of native, pulped and hydrolyzed palm residues; namely: fronds, leaves, and coir.

	Fronds	Leaves	Coir
Native	28	29	31
Pulp	33	30	32
CNC	–	27	–

4. Conclusion

For fronds, leaves, and coir, our preparation technique was successful to isolate lignin containing nanocellulose.

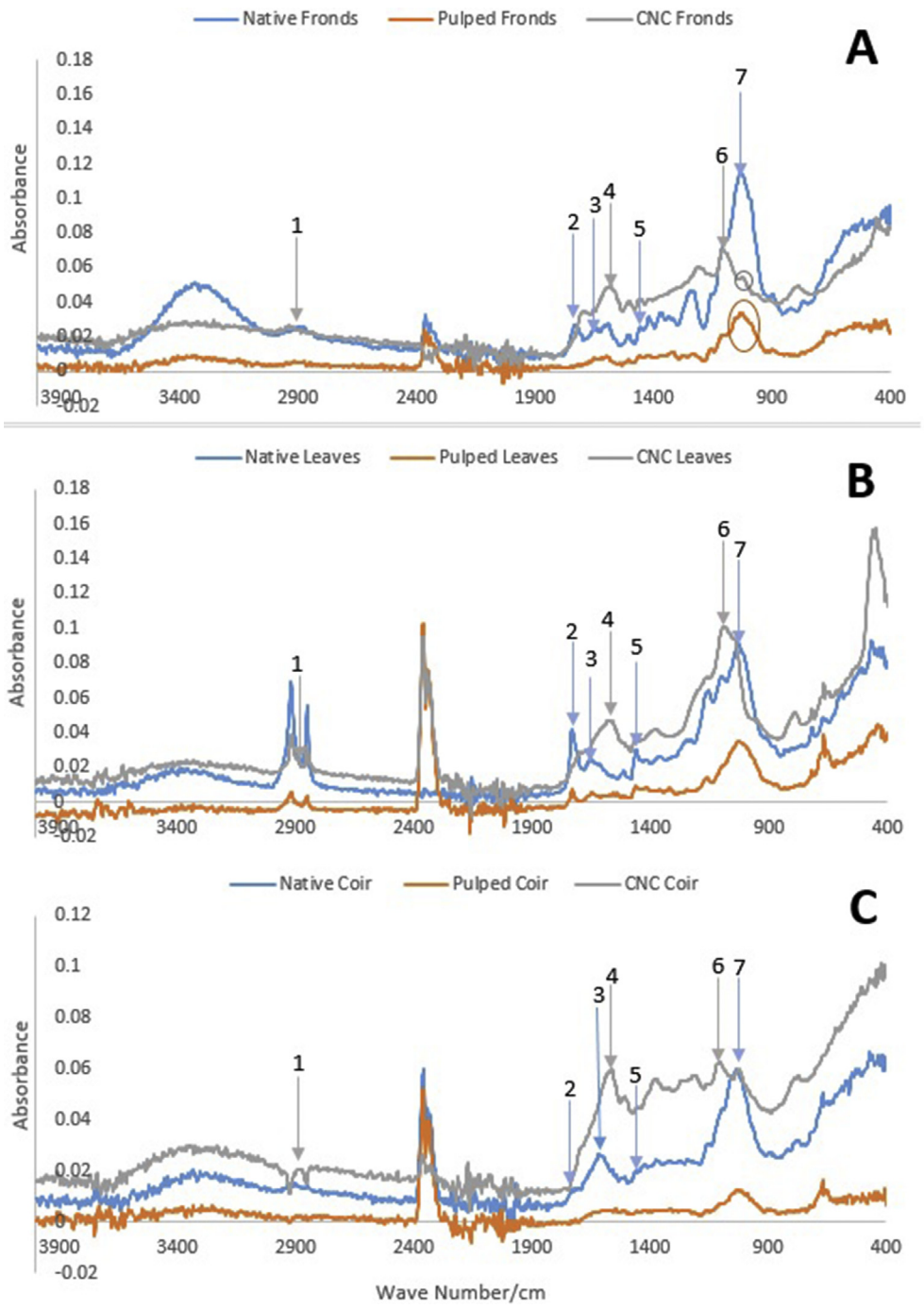

Fig. 5 – FTIR spectroscopy for the three types of palm residues A) fronds, B) leaves, and C) coir.

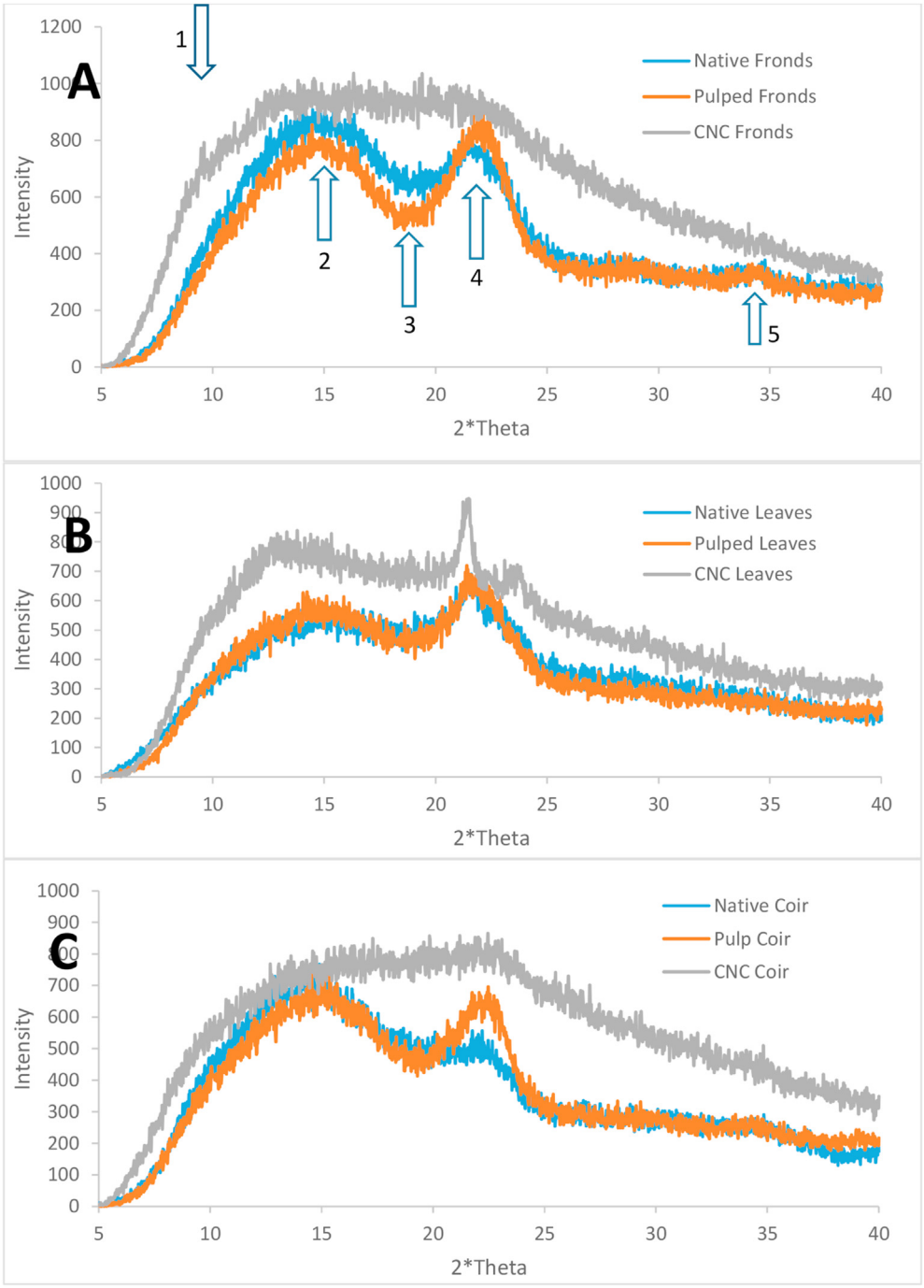

Fig. 6 – XRD analysis of three types of palm residues A) fronds, B) leaves, and C) coir. The three residues were characterized in native, pulped, and hydrolyzed states.

Table 5 – Nanocellulose extraction methods and properties, with emphasis on palm residues.

	Step 1	Step 2	Step 3	Results 1	Results 2	Ref.
Palm fruit bunch fibers	Bleaching 0.7% w/v NaClO2 2hrs (4 times)	Pulping 17.5% (w/v) NaOH	Acidic hydrolysis 64 wt% H_2SO_4 under strong agitation at 45C for 45 min	Shape nano whisker Size CNC width ranges 4–14 nm	FTIR Lignin peaks disappeared Crystallinity CI of native 38% CI of CNC 73%	[46]
Palm leaves fibers	Bleaching $NaClO_2$ reflux for 5 times	Pulping 17.5% (w/v) NaOH 5 h	Acidic hydrolysis 9M H_2SO_4 5h (10ml/gm)	Shape nano whisker 16–23 nm	FTIR Lignin peaks disappeared and OH peaks are sharper (smaller size) Crystalliniyu CI native 23.4%, CI CNC 70%	[47]
Palm outer sheath	Pulping 5% NaOH wt/dry fiber	Bleaching 1.5 gm NaClO2 + 160 ml water (Step 1+ step 2) are repeated 3 times	Mechanical extraction Homogenizer Defibrillator (grinder)	Shape nano fibrils	FTIR Lignin peaks disapeared Crystallinity CI native 21% CI of CNF 50%	[48]
Palm fruit bunch fibers	Pulping 10% wt. NaOH	Acidic hydrolysis H_2SO_4 36% (or) H_3PO_4 62%	Homogenizer (20,000 rpm)	shape nano whisker width 9.6–12.5 nm		[49]
Luffa cylindrica	Cryocrushing+ Soxlet extraction	enzymatic hydrolysis (cellulose+pictenase)		Shape Cuboidal particles Size 50–100 nm	FTIR Cellulose peaks disappeared and OH peaks are sharper (smaller size) Crystallinity CI native 67.9%, CI hydrolyzed 51%	[50]

However, coir was less compliant to acidic hydrolysis. The three types yielded 42–82 nm spherical particles, and zeta potential ranging between −11 and −19 mV. Crystallinity was higher after pulping, and lower after hydrolysis. This suggests the promotion of amorphous content of cellulose. Our palm based lignin-containing nano particles open up whole new field of material development, especially in heavy metal (cations) removal from water for environmental applications.

Declaration of Competing Interest

The authors declare that they have no known competing financial interests or personal relationships that could have appeared to influence the work reported in this paper.

Acknowledgements

This paper and the research behind it would have been impossible to deliver, without the financial support from European Union under umbrella of Erasmus+ KA107 PhD Mobility scheme. Moreover, I would like to acknowledge Furthermore, I would like to appreciate Dept. Chair in Granada Dr. Jose Maria Moreno and his kind secretary Antonio de la Torra.

REFERENCES

[1] Kumar R, Singh S, Singh OV. Bioconversion of lignocellulosic biomass: biochemical and molecular perspectives. J Ind Microbiol Biotechnol 2008;35(5):377–91.
[2] Mehanny S, Farag M, Rashad RM, Elsayed H. Fabrication and characterization of starch based bagasse fiber composite [Internet]. In: Design, materials and manufacturing, parts A, B, and C, Vol. 3. ASME; 2012. p. 1345 [cited 2016 Aug 7]. Available from: http://proceedings.asmedigitalcollection.asme.org/proceeding.aspx?doi=10.1115/IMECE2012-86265.
[3] Mehanny S, Darwish L, Ibrahim H, El-Wakad MT, Farag M. High-content lignocellulosic fibers reinforcing starch-based biodegradable composites: properties and applications. In: Composites from renewable and sustainable materials. InTech; 2016.
[4] Mehanny S, Darwish L, Abd El Haleem M, El-Kashif E, Farag M, Ibrahim H. Effect of glue and temperatures on mechanical properties of starch-based biodegradable composites reinforced with bagasse fibers. Int J Biotechnol Biomater Eng 2019;1(1).
[5] Ibrahim MM, Moustafa H, Rahman ENAEL, Mehanny S, Hemida MH, El-Kashif E. Reinforcement of starch based biodegradable composite using Nile rose residues. J Mater Res Technol May–June 2020;9(3):6160–71.
[6] Väisänen T, Haapala A, Lappalainen R, Tomppo L. Utilization of agricultural and forest industry waste and residues in natural fiber-polymer composites: a review. Waste Manag 2016;54:62–73.
[7] Ashori A. Municipal solid waste as a source of lignocellulosic fiber and plastic for composite industries. Polym Plast Technol Eng 2008;47(8):741–4.
[8] Kumar P, Barrett DM, Delwiche MJ, Stroeve P. Methods for pretreatment of lignocellulosic biomass for efficient hydrolysis and biofuel production. Ind Eng Chem Res 2009;48(8):3713–29.
[9] El-Juhany Loutfy I. Degradation of date palm trees and date production in Arab countries: causes and potential rehabilitation. Aust J Basic Appl Sci 2010;4(8):3998–4010.
[10] Nasser RA, Salem MZM, Hiziroglu S, Al-Mefarrej HA, Mohareb AS, Alam M, et al. Chemical analysis of different parts of date palm (Phoenix dactylifera L.) using ultimate, proximate and thermo-gravimetric techniques for energy production. Energies 2016;9(5):374.
[11] Siqueira G, Bras J, Dufresne A. New process of chemical grafting of cellulose nanoparticles with a long chain isocyanate. Langmuir 2010;26(1):402–11.
[12] Börjesson M, Westman G. Crystalline nanocellulose—preparation, modification, and properties. In: Cellulose-fundamental aspects and current trends. InTech; 2015.
[13] Dufresne A. Cellulose nanomaterial reinforced polymer nanocomposites. Curr Opin Colloid Interface Sci 2017;29:1–8.
[14] Sheltami RM, Kargarzadeh H, Abdullah I, Ahmad I. Thermal properties of cellulose nanocomposites. In: Handb nanocellulose Cellul nanocomposites, vol. 2; 2017. p. 523–52.
[15] Österberg M, Vartiainen J, Lucenius J, Hippi U, Seppälä J, Serimaa R, et al. A fast method to produce strong NFC films as a platform for barrier and functional materials. ACS Appl Mater Interfaces 2013;5(11):4640–7.
[16] Camarero-Espinosa S, Endes C, Mueller S, Petri-Fink A, Rothen-Rutishauser B, Weder C, et al. Elucidating the potential biological impact of cellulose nanocrystals. Fibers 2016;4(3):21.
[17] Favier V, Canova GR, Cavaillé JY, Chanzy H, Dufresne A, Gauthier C. Nanocomposite materials from latex and cellulose whiskers. Polym Adv Technol 1995;6(5):351–5.
[18] Desmaisons J, Gustafsson E, Dufresne A, Bras J. Hybrid nanopaper of cellulose nanofibrils and PET microfibers with high tear and crumpling resistance. Cellulose 2018;25(12):7127–42.
[19] Hubbe MA, Ferrer A, Tyagi P, Yin Y, Salas C, Pal L, et al. Nanocellulose in thin films, coatings, and plies for packaging applications: a review. BioResources 2017;12(1):2143–233.
[20] Dufresne A. Nanocellulose processing properties and potential applications. Curr For Rep 2019;5(2):76–89.
[21] Dufresne A. Nanocellulose: from nature to high performance tailored materials. Walter de Gruyter GmbH & Co KG; 2017.
[22] Mohamed MA, Abd Mutalib M, Hir ZAM, Zain MFM, Mohamad AB, Minggu LJ, et al. An overview on cellulose-based material in tailoring bio-hybrid nanostructured photocatalysts for water treatment and renewable energy applications. Int J Biol Macromol 2017;103:1232–56.
[23] Turbak AF, Snyder FW, Sandberg KR. Microfibrillated cellulose, a new cellulose product: properties, uses, and commercial potential. In: J appl polym sci: appl polym symp;(United States); 1983.
[24] Boerjan W, Ralph J, Baucher M. Lignin biosynthesis. Annu Rev Plant Biol 2003;54(1):519–46.
[25] Jouanin L, Lapierre C. Lignins: biosynthesis, biodegradation and bioengineering, vol. 61. Academic Press; 2012.
[26] Lu H, Zhang L, Liu C, He Z, Zhou X, Ni Y. A novel method to prepare lignocellulose nanofibrils directly from bamboo chips. Cellulose 2018;25(12):7043–51.
[27] Upton BM, Kasko AM. Strategies for the conversion of lignin to high-value polymeric materials: review and perspective. Chem Rev 2016;116(4):2275–306.
[28] Mandal A, Chakrabarty D. Isolation of nanocellulose from waste sugarcane bagasse (SCB) and its characterization. Carbohydr Polym 2011;86(3):1291–9.
[29] Fahma F, Iwamoto S, Hori N, Iwata T, Takemura A. Isolation, preparation, and characterization of nanofibers from oil palm empty-fruit-bunch (OPEFB). Cellulose 2010;17(5):977–85.

[30] Prathapan R, Thapa R, Garnier G, Tabor RF. Modulating the zeta potential of cellulose nanocrystals using salts and surfactants. Colloids Surf A Physicochem Eng Asp 2016;509:11–8.
[31] Mohaiyiddin MS, Lin OH, Owi WT, Chan CH, Chia CH, Zakaria S, et al. Characterization of nanocellulose recovery from Elaeis guineensis frond for sustainable development. Clean Technol Environ Policy 2016;18(8):2503–12.
[32] Yang X, Han F, Xu C, Jiang S, Huang L, Liu L, et al. Effects of preparation methods on the morphology and properties of nanocellulose (NC) extracted from corn husk. Ind Crop Prod 2017;109:241–7.
[33] Morais JPS, de Freitas Rosa M, Nascimento LD, do Nascimento DM, Cassales AR, others. Extraction and characterization of nanocellulose structures from raw cotton linter. Carbohydr Polym 2013;91(1):229–35.
[34] Šurina I, Jablonsk\'y M, Ház A, Sladková A, Briškárová A, Kač\'\ik F, et al. Characterization of non-wood lignin precipitated with sulphuric acid of various concentrations. BioResources 2015;10(1):1408–23.
[35] Lievonen M, Valle-Delgado JJ, Mattinen M-L, Hult E-L, Lintinen K, Kostiainen MA, et al. A simple process for lignin nanoparticle preparation. Green Chem 2016;18(5):1416–22.
[36] Yang H, Yan R, Chen H, Lee DH, Zheng C. Characteristics of hemicellulose, cellulose and lignin pyrolysis. Fuel 2007;86(12–13):1781–8.
[37] Alvarez VA, Vázquez A. Influence of fiber chemical modification procedure on the mechanical properties and water absorption of MaterBi-Y/sisal fiber composites. Compos Part A Appl Sci Manuf 2006;37(10):1672–80.
[38] Oh SY, Yoo D Il, Shin Y, Seo G. FTIR analysis of cellulose treated with sodium hydroxide and carbon dioxide. Carbohydr Res 2005;340(3):417–28.
[39] Nelson ML, O'Connor RT. Relation of certain infrared bands to cellulose crystallinity and crystal lattice type. Part II. A new infrared ratio for estimation of crystallinity in celluloses I and II. J Appl Polym Sci 1964;8(3):1325–41.
[40] Ilyas RA, Sapuan SM, Ishak MR. Isolation and characterization of nanocrystalline cellulose from sugar palm fibres (Arenga Pinnata). Carbohydr Polym 2018;181:1038–51.
[41] Shi J, Shi SQ, Barnes HM, Pittman Jr CU, others. A chemical process for preparing cellulosic fibers hierarchically from kenaf bast fibers. BioResources 2011;6(1):879–90.
[42] C\uAPRARU A-M, Popa VI, M\uALU\cTAN T, LIS\uA G. Contribution to the modification and characterization of different types of lignins. 2009.
[43] Mora JI. Extraction of cellulose and preparation of nanocellulose from sisal fibers. 2008. p. 149–59.
[44] Park S, Baker JO, Himmel ME, Parilla PA, Johnson DK. Cellulose crystallinity index: measurement techniques and their impact on interpreting cellulase performance. Biotechnol Biofuels 2010;3(1):10.
[45] Nilsson C. Preparation and characterization of nanocellulose from wheat bran. 2017.
[46] Lani NS, Ngadi N, Johari A, Jusoh M. Isolation, characterization, and application of nanocellulose from oil palm empty fruit bunch fiber as nanocomposites. J Nanomater 2014;2014.
[47] Elias N, Chandren S, Attan N, Mahat NA, Razak FIA, Jamalis J, et al. Structure and properties of oil palm-based nanocellulose reinforced chitosan nanocomposite for efficient synthesis of butyl butyrate. Carbohydr Polym 2017;176:281–92.
[48] Franco TS, Potulski DC, Viana LC, Forville E, de Andrade AS, de Muniz GIB. Nanocellulose obtained from residues of peach palm extraction (Bactris gasipaes). Carbohydr Polym 2019;218:8–19.
[49] Septevani AA, Rifathin A, Sari AA, Sampora Y, Ariani GN, Sondari D, et al. Oil palm empty fruit bunch-based nanocellulose as a super-adsorbent for water remediation. Carbohydr Polym 2020;229:115433.
[50] Rangan A, Manchiganti MV, Thilaividankan RM, Kestur SG, Menon R. Novel method for the preparation of lignin-rich nanoparticles from lignocellulosic fibers. Ind Crop Prod 2017;103:152–60.
[51] Huang Y, Nair SS, Chen H, Fei B, Yan N, Feng Q. Lignin-rich nanocellulose fibrils isolated from parenchyma cells and fiber cells of western red cedar bark. ACS Sustain Chem Eng 2019;7(18):15607–16.
[52] Figueiredo P, Lintinen K, Hirvonen JT, Kostiainen MA, Santos HA. Properties and chemical modifications of lignin: towards lignin-based nanomaterials for biomedical applications. Prog Mater Sci 2018;93:233–69.
[53] Agrawal A, Kaushik N, Biswas S. Derivatives and applications of lignin–an insight. SciTech J 2014;1(7):30–6.
[54] Bayoumi Ashraf, Sarg Marwa, Fahmy Tamer, Mohamed Noha, El-Zawawy Waleed. The behavior of natural biomass materials as drug carriers in releasing loaded Gentamicin sulphate. Arab J Chem 2020;13(12):8920–34. https://doi.org/10.1016/j.arabjc.2020.10.018. In press.
[55] Mehanny Sherif, Ibrahim Hamdy, Darwish Lamis, Farag Mahmoud, El-Habbak Abdel-Halim, El-Kashif Emad. Effect of environmental conditions on date palm fiber composites. Singapore: Springer; 2020. p. 287–320.